

# Preparation of nano-size $ZrB_2$ powder by self-propagating high-temperature synthesis

H. Erdem Çamurlu<sup>a,\*</sup>, Filippo Maglia<sup>b,1</sup>

<sup>a</sup> Mechanical Engineering Department, Akdeniz University, Dumlupınar Bulvarı, Kampus, 07058 Antalya, Turkey

<sup>b</sup> Department of Physical Chemistry, University of Pavia, V.le Taramelli 16, 26100 Pavia, Italy

Received 4 July 2008; received in revised form 4 September 2008; accepted 13 September 2008

Available online 19 October 2008

## Abstract

Preparation of nano-size  $ZrB_2$  powder by SHS has been investigated. Zr and B elemental powders were mixed with 10–50 wt.% NaCl, and prepared pellets were reacted under argon. Adiabatic temperatures were calculated by HSC software. Increasing NaCl content led to a continuous decrease in adiabatic temperatures and reaction wave velocity. Products were subjected to XRD, SEM and FESEM analyses. Average crystallite size of  $ZrB_2$ , which was 303 nm without NaCl, decreased to 32 nm with 40% NaCl addition. Distinct decrease in  $ZrB_2$  particle size was also observed from SEM analyses. 30% NaCl addition was found to be optimum for ensuring a stable SHS reaction and providing the formation of nano-size  $ZrB_2$  particles. It was revealed from particle size distribution measurements that  $ZrB_2$  powder obtained by 30 wt.% NaCl addition contained particles mostly finer than 200 nm. A mechanism, similar to solution-precipitation was proposed for the particle size refining effect of NaCl.

© 2008 Elsevier Ltd. All rights reserved.

**Keywords:** Powders-chemical preparation; Grain size; Borides; Refractories; SHS

## 1. Introduction

Zirconium diboride ( $ZrB_2$ ) is one of the most stable borides.<sup>1</sup> It is in ultrahigh-temperature ceramics class with a melting point of as high as 3050 °C. It has outstanding wear and corrosion resistance, high heat and electrical conductivity, and high hardness.<sup>2</sup> Possible applications of  $ZrB_2$  bearing ceramics involve cutting tools, crucibles for molten metal handling, high-temperature electrodes and high-temperature spray nozzles.<sup>1–3</sup>  $ZrB_2$  has been produced through various methods starting from elemental Zr or its oxide,  $ZrO_2$ . Reaction between Zr and B elemental powders, metallothermic reduction of  $ZrO_2$  and  $B_2O_3$  by magnesium or boron,<sup>4,5</sup> fused salt electrolysis,<sup>6</sup> mechanochemical synthesis and combustion synthesis<sup>7</sup> are some of the methods.

In the last decade, there has been a growing appeal on the production of ceramic powder having ultrafine or nano-sized particles and nano-grained sintered particles. Exceptional properties such as excellent sinterability of nano-powder and improved mechanical properties of the formed nano-grained particles are the motivation for this appeal.<sup>8,9</sup> In this respect SHS is quite challenging due to the high temperatures involved that lead to considerable grain coarsening in the product. Formation of nano-sized powder through SHS has been investigated by various groups.<sup>10–13</sup> For this purpose, effect of addition of diluents into the reactants, which are mostly preformed powder of the same kind as the expected products, has been investigated.<sup>13</sup> However, the simple use of the product as a diluent did not provide sufficient grain refinement and the formation of submicron size particles is not achieved in most cases.<sup>12</sup> The use of volatile species as diluent has been recently suggested as an alternative method. Specifically, in the case of the SHS leading to the formation of borides and carbides, NaCl has been employed.<sup>10–12</sup> Nanometric  $TiB_2$  powder was reported to be produced through SHS using  $H_3BO_3$ , Mg and  $TiO_2$ , and NaCl as the diluent.<sup>11</sup> Grain refinement, due to addition of NaCl, has also been reported in the combustion synthesis of TiC from Ti and C powders.<sup>12</sup> Starting powder mixtures containing  $H_3BO_3$ ,  $ZrO_2$  and Mg have

\* Corresponding author at: Makine Mühendisliği Bölümü, Akdeniz Üniversitesi, Dumlupınar Bulvarı, Kampüsü, 07058 Antalya, Türkiye. Tel.: +90 242 310 6346 fax: +90 242 310 6306.

E-mail address: [erdemcamurlu@gmail.com](mailto:erdemcamurlu@gmail.com) (H.E. Çamurlu).

<sup>1</sup> Dipartimento di Chimica Fisica, Università di Pavia, Viale Taramelli 16, 27100 Pavia, Italia.

been used for the synthesis of  $ZrB_2$  by SHS and it was stated that addition of NaCl resulted in a decrease in the particle size of the formed  $ZrB_2$ .<sup>10</sup> However, utilization of oxide starting materials not only results in formation of side products like magnesium borates that require further removal steps such as acid leaching; but also decrease the efficiency of the reactions.<sup>7,14</sup> Additionally, residual  $ZrO_2$  remains in the products in spite of the precautions including utilization of sub-stoichiometric amount of  $ZrO_2$  in the starting mixture.<sup>15</sup> Unreacted  $ZrO_2$  in the products cannot be removed from  $ZrB_2$  due to its insolubility in acid solutions.<sup>7,15</sup> Consequently, starting from elemental Zr and B powders was found to be more advantageous and is the topic of the present study.

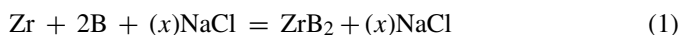
In the present study, SHS preparation of nano-size  $ZrB_2$  powder has been investigated from Zr and B elemental starting powders with NaCl additions. Increased surface area of the nano-size powder obtained by this technique is expected to provide sintering at lower temperatures and also bring about better mechanical properties of the sintered parts, as compared to micron-scale powder.<sup>8</sup>

## 2. Experimental procedure

Preparation of  $ZrB_2$  from mixtures of elemental Zr (Alfa Aesar, 95%), elemental amorphous B (Alfa Aesar, 90%) and NaCl (Merck Chemicals) through SHS has been investigated. According to SEM observations Zr powder was composed of particles having 1–3  $\mu m$  size and B particles were smaller than 1  $\mu m$ .<sup>16</sup> Starting materials in powder form were weighed in stoichiometric proportions according to reaction (1) then dry mixed and ground thoroughly in an agate mortar and pestle. NaCl (Merck Chemicals) was added to Zr–B mixtures in 10–50% weight ratio with 10 wt.% increments. The powder mixtures were pressed in the form of 10 mm high cylindrical pellet with a diameter of 8 mm and % theoretical density of 50–55.

Two reasons were considered for the utilization of NaCl as a diluent. First, NaCl does not react with the starting materials and it is believed to have the possibility to develop a layer among forming  $ZrB_2$  crystals thereby preventing their growth by separating them from each other. Second reason is the ease in separation of NaCl from the products, due to its high solubility in water.<sup>12</sup>

Adiabatic temperatures of the mixtures containing increasing amounts of NaCl according to reaction (1) were calculated by the HSC software.<sup>17</sup>



The reacting pellets were placed inside a stainless steel reactor and the SHS process was ignited by an electrically heated tungsten coil placed at a distance of 1.0 mm from the top surface of the pellet. All experiments were conducted in a high purity argon (99.998%) atmosphere. Video recordings of the reaction were used to measure the reaction velocity.

Products obtained after SHS reactions were subjected to X-ray powder diffraction (XRPD) analyses (Bruker D8 Advance) with  $Cu K\alpha$  radiation. Average crystallite size of  $ZrB_2$  crys-

tals obtained by using various amounts of NaCl was calculated according to Scherrer formulae, making use of the widths of the peaks on XRPD patterns.<sup>18</sup> In these calculations, the measured peak widths were corrected by removing the instrumental line broadening, which was obtained by utilizing a  $BaF_2$  reference sample.<sup>18</sup> Particle size and morphology of the products were examined by scanning electron microscope (SEM, Cambridge Stereoscan 200). In order to remove the NaCl from  $ZrB_2$  particles, product pellets were crushed and ground in an agate mortar and pestle. NaCl in the obtained powder was dissolved in distilled water at room temperature and the slurry was centrifuged at 3000 rpm (Misral 2000) for 3 min to separate the fine  $ZrB_2$  particles by sedimentation. Filtering could not be utilized for solid–liquid separation because of the possibility of losing fine particles, which pass through the filter. After decantation, the residue containing sediment  $ZrB_2$  particles were dried. They were subjected to further SEM (Zeiss Leo 1430), field emission scanning electron microscope (FESEM, JEOL 6335F), and particle size distribution analyses (Malvern Instruments, Zetasizer Nano-ZS).

## 3. Results and discussion

Adiabatic temperatures of the Zr–B mixtures containing 0–50 wt.% NaCl according to reaction (1) were calculated by HSC software, and they are presented in Fig. 1. The calculated adiabatic temperature for the undiluted reaction (1) is equal to the  $ZrB_2$  melting point (3050 °C). The adiabatic temperature was not lowered for NaCl additions up to 10 wt.% although a decrease in the fraction of molten  $ZrB_2$  in the product should occur as well as a decrease in the actual ‘real temperature’ which is predictably lower than the adiabatic value due to heat losses and therefore not thermodynamically bound to the melting point

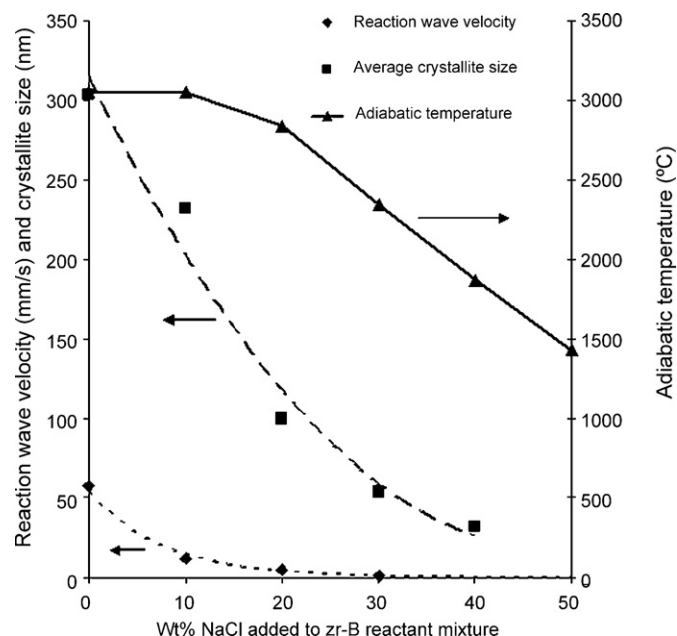


Fig. 1. Adiabatic temperatures, propagation velocity of the reaction wave, and average crystallite size of the formed  $ZrB_2$ .

value. Addition of amounts of NaCl higher than 10 wt.% results, on the other hand, in a considerable decrease in the adiabatic temperature of the reaction.

Combustion wave velocities of pellets containing varying amounts of NaCl were calculated by means of the records taken during reactions. Results are presented in Fig. 1. A planar steady state reaction front was observed for low NaCl contents with a sharply decreasing velocity as the amount of NaCl is increased from 0% (front velocity 57 mm/s) to 30% (front velocity 1.1 mm/s). At 40 wt.% of NaCl the propagation of the combustion reaction becomes unsteady and a velocity value cannot be properly measured. At 50 wt.% NaCl the reaction could not be ignited. These observations are in agreement with the calculated adiabatic temperature value: reactions characterized by adiabatic temperatures below 1800 K are expected to be non-steady or non-propagating.<sup>19</sup>

The pellets obtained after SHS reactions had layered structure with very high porosity, and they could be ground in a mortar and pestle into powder form. Products formed by NaCl additions were seen to be more fragile and easier to grind than the ones obtained without NaCl, most probably due to less amount of sin-

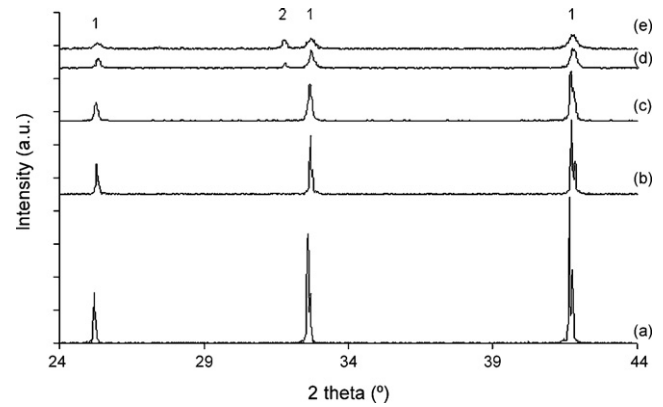


Fig. 2. XRD patterns of the products obtained from Zr–B mixtures containing: (a) 0 wt.%, (b) 10 wt.%, (c) 20 wt.% NaCl, (d) 30 wt.%, (e) 40 wt.% NaCl after SHS reactions. (1)  $ZrB_2$  and (2) NaCl.

tering caused by decreased adiabatic temperatures and presence of NaCl among the particles.

The XRD patterns of samples with initial content of NaCl from 0 to 40% are reported in Fig. 2. In all cases  $ZrB_2$  and

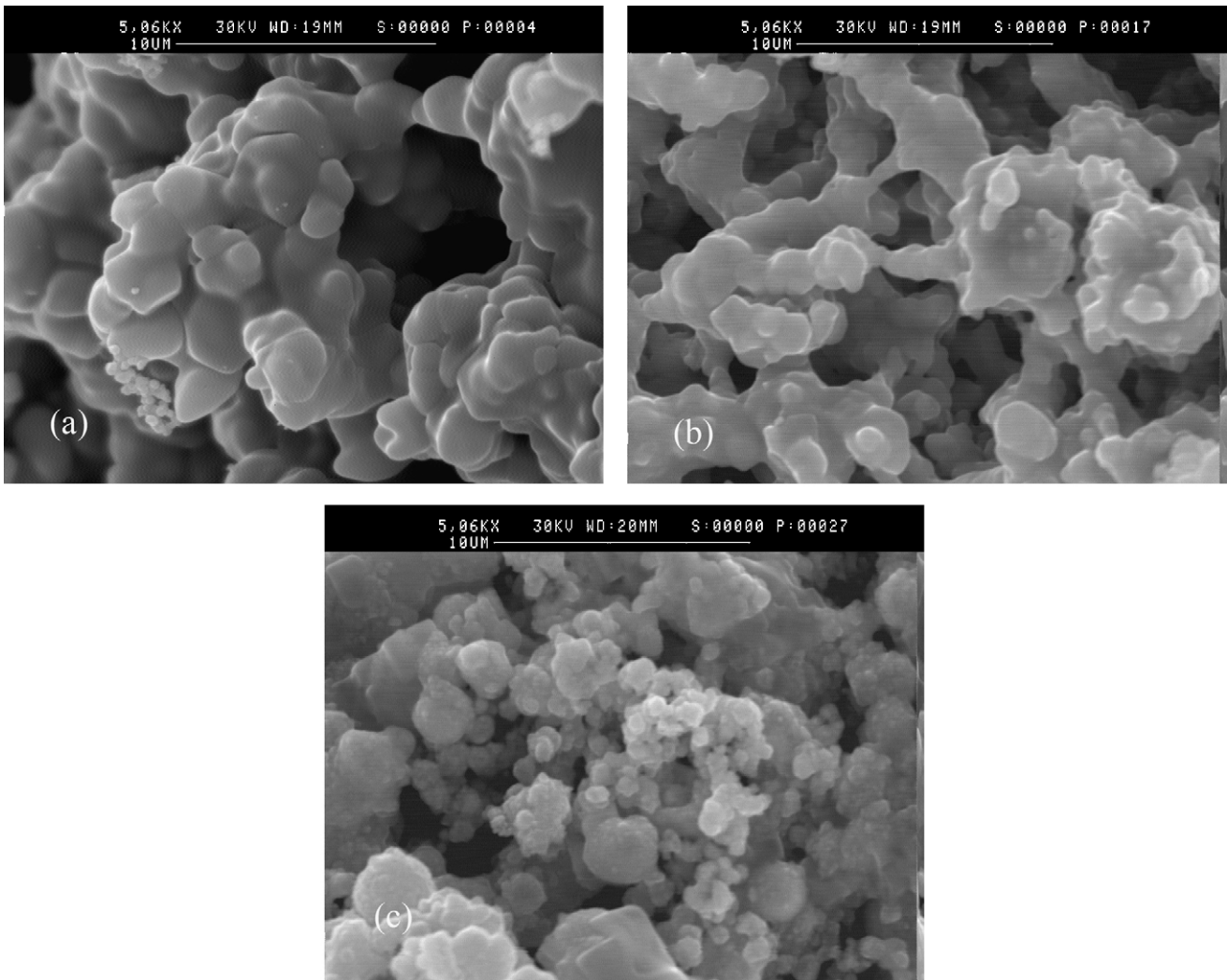


Fig. 3. SEM micrographs of the fracture surfaces of the products obtained from Zr–B mixtures containing (a) 0 wt.% NaCl, (b) 10 wt.% NaCl, and (c) 30 wt.% NaCl.



NaCl (peaks belonging to NaCl can be observed when the NaCl in the starting mixture is above 20%) were the only products. It can be concluded that, not only complete conversion of the reactants into products was obtained even in samples with high NaCl content, but also the formation of undesired phase such as  $ZrO_2$  was prevented.

The width of the diffraction peaks belonging to  $ZrB_2$  increase with the NaCl content in the starting mixture (Fig. 2(b–e)) as an effect of the decrease of the average crystallite size of  $ZrB_2$  as the reaction temperature is lowered. The average crystallite sizes of  $ZrB_2$ , calculated by the Scherrer formulae, are shown in Fig. 1. A sharp decrease of approximately one order of magnitude (from 300 to 30 nm) was obtained by lowering the adiabatic temperature from 3050 to 1870 °C.

SEM micrographs of the fracture surfaces of the product pellets obtained with 0, 10 and 30 wt.% NaCl contents are shown in Fig. 3. Trends in the product morphology are clearly observable. The particle size of  $ZrB_2$  decreased from about 2–4  $\mu\text{m}$  (Fig. 3(a)) for the highest combustion temperature, to sub-micron values (Fig. 3(c)) for the lowest combustion temperature. The level of particle coarsening was highest for the lowest NaCl

contents, as expected on the basis of the adiabatic temperature. For NaCl up to 10 wt.% the product morphology suggests the presence of partial melting (Fig. 3(a and b)). Increase in the NaCl amount further reduced the particle size. Microstructures of the products were similar and there was no sign of melting or fusion of  $ZrB_2$  particles for NaCl contents higher than 10 wt.% NaCl. However, bulky and round shaped formations could be observed in the products of these samples (Fig. 3(c)). In XRD analyses residual NaCl was found to be present in the products when NaCl content was higher than 20 wt.%. It appears therefore that the growth of round shaped powder as observed in SEM study is due to the presence of NaCl in the synthesized powder, which indicates that all the NaCl is not evaporated. As was observed in the case of the synthesis of  $TiB_2$ ,<sup>11</sup> NaCl in the product phase is most probably located as a coating on the formed  $ZrB_2$  grains' surface. The formed  $ZrB_2$  grains are possibly surrounded by NaCl and are embedded in the round shaped formations of NaCl. This indeed is believed to play a key role in the refining of the  $ZrB_2$  particle size by keeping apart the  $ZrB_2$  grains. On the other hand, it prevents a precise evaluation of the particle size of  $ZrB_2$ . For that reason NaCl was removed by

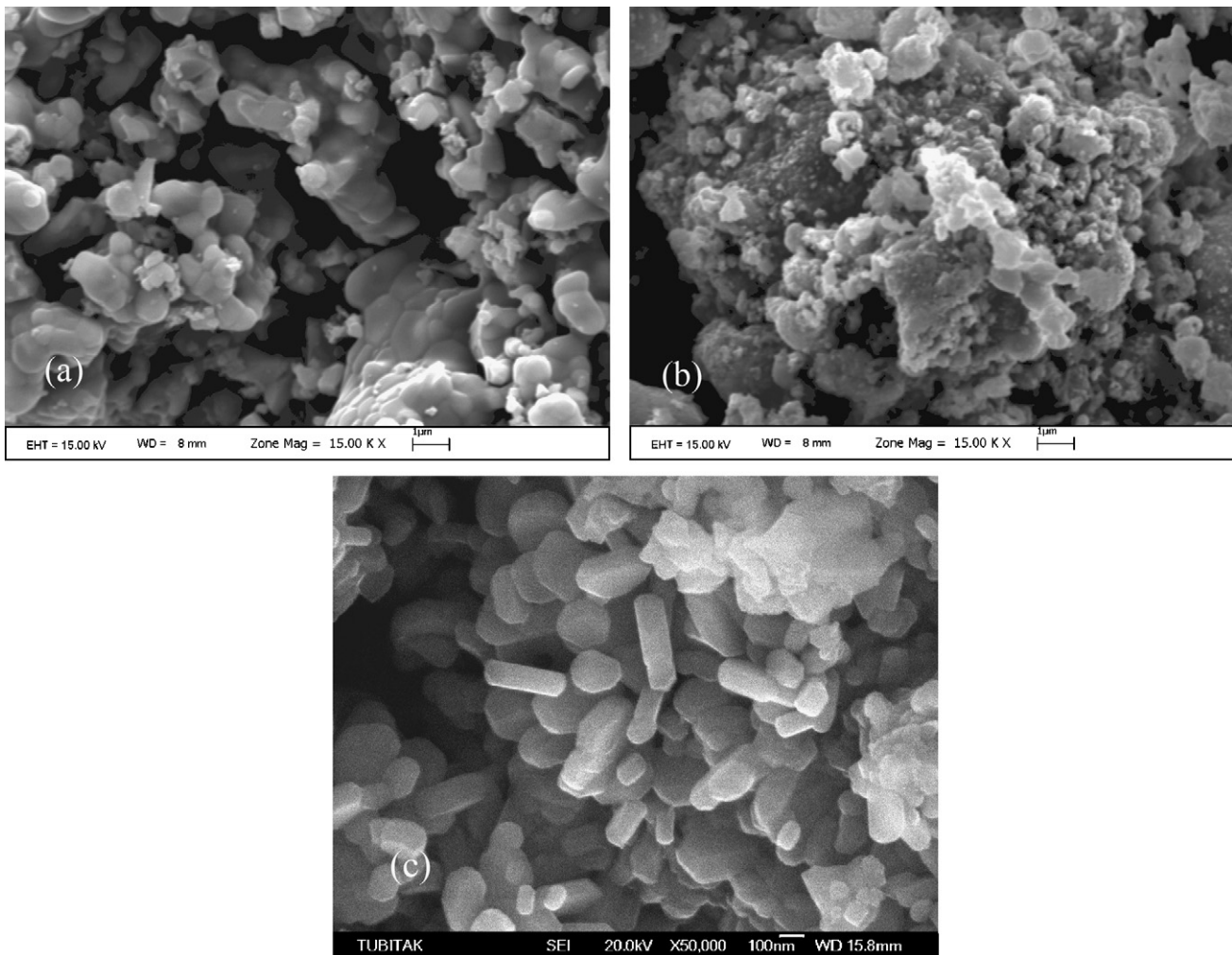


Fig. 4. (a), (b) SEM and (c) FESEM micrographs of the  $ZrB_2$  powder after NaCl removal. Products were obtained from Zr–B mixtures containing (a) 10 wt.% NaCl, (b) and (c) 30 wt.% NaCl.

dissolving in water. Pure  $ZrB_2$  particles were obtained after centrifuging the slurry at 3000 rpm for 3 min, decanting and drying. NaCl free  $ZrB_2$  particles were then subjected to further SEM analyses and particle size measurement.

High magnification SEM micrographs of  $ZrB_2$  powder obtained after NaCl removal are given in Fig. 4. The samples that originally contained low NaCl amounts (up to 10 wt.%) were still composed of agglomerates of sintered grains even after grinding as can be seen in Fig. 4(a). The agglomerates were in various sizes, as a result of grinding in mortar and pestle. They were mostly in the range of 2–5  $\mu\text{m}$  and apparently larger in the products which were obtained without NaCl addition. For higher NaCl contents than 10 wt.%, the powders were on the other hand made of soft agglomerates. Thanks to the removal of NaCl it is now possible to observe (Fig. 4(b and c)) that a significant reduction in the particle size of  $ZrB_2$  was achieved when large amounts of NaCl were added to the starting mixture. The average particle size was reduced from approximately 1  $\mu\text{m}$  at 10 wt.% NaCl to a scale of 100 nm at 30 wt.% NaCl. Particle size of  $ZrB_2$  as measured from SEM micrographs is as usual larger than the average crystallite size calculated by the Scherrer formulae due to the polycrystalline structure of  $ZrB_2$  particles. Formed  $ZrB_2$  particles appear to have faceted morphology and they are hexagonal in shape (Fig. 4(c)), which is possibly an imposition of the hexagonal close packed crystal structure of  $ZrB_2$ .

To obtain a precise estimation of the particle size and particle size distribution, measurements by zeta potential after NaCl removal were performed on all samples.  $ZrB_2$  powder obtained from pure and 10 wt.% NaCl mixtures yielded, as expected, to incorrect results due to the hard agglomerations.  $ZrB_2$  powders obtained from 20 and 30 wt.% NaCl mixtures exhibited similar particle size distributions. Particle size distribution graph of  $ZrB_2$  powder obtained from Zr–B mixture containing 30 wt.% NaCl is given in Fig. 5. The results are in fairly good agreement with the cursory estimation made on the basis of SEM images. Most of the  $ZrB_2$  powder was composed of particles with size between 70 and 200 nm. Product obtained by 30 wt.%

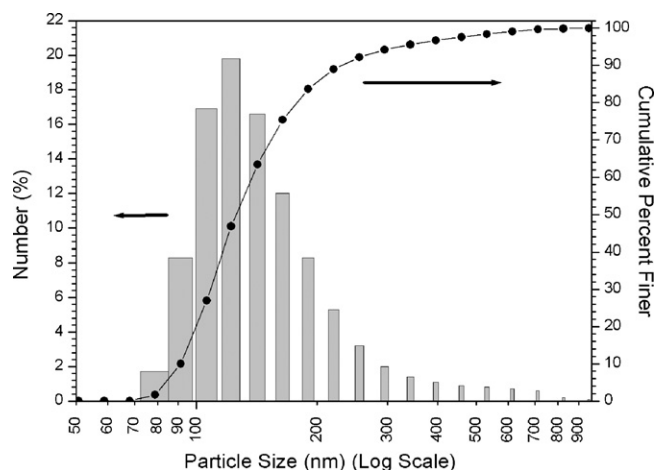


Fig. 5. Particle size distribution of  $ZrB_2$  powder obtained from Zr–B mixture containing 30 wt.% NaCl.

Table 1  
Melting and boiling points of the reactants and products<sup>12,17,20</sup>.

	Zr	B	NaCl	$ZrB_2$
$T_m$ ( $^{\circ}\text{C}$ )	1855	2075	801	3050
$T_b$ ( $^{\circ}\text{C}$ )	4409	4000	1465	

NaCl addition contained more particles finer than 100 nm than the powder obtained by 20 wt.% NaCl addition. It should be noted that the particle size values obtained by zeta potential measurements include values of additional hydrate layer around  $ZrB_2$  particles, thus the particles are expected to be smaller than the data given in Fig. 5, and a higher percentage than the data given in Fig. 5 is likely to be <100 nm.

Formation of TiC from Ti–C–NaCl mixtures through SHS was investigated by Nersisyan et al.<sup>12</sup> They proposed that Ti and NaCl, which are expected to be at liquid state at the reaction temperature, form a melt that covers the solid carbon particles. In this system that is chemically very active, carbonization of liquid titanium takes place resulting in formation of TiC particles. A similar mechanism to that proposed for Ti–C system may apply to Zr–B compositions containing NaCl. According to the adiabatic temperatures of reactions given in Fig. 1 and melting points of the reactants given in Table 1, in the NaCl free sample first Zr and then B are expected to melt in the preflame zone ahead of the reaction wave. Therefore, it is safe to say that the reaction takes place between liquid Zr and B reactants. In the case of NaCl containing samples, melting and vaporization of NaCl is expected to take place prior to melting of Zr and B in the preflame zone regarding to its much lower melting and vaporization point than melting points of Zr and B. Presence of NaCl, as verified by the XRD analyses, may be attributed to building up and trapping of NaCl vapor inside the pores of the reaction pellet and suppression of vaporization of NaCl. Calculated adiabatic temperatures are higher than the melting temperatures of Zr and B for all compositions containing less NaCl than 40 wt.%. Ahead of the reaction zone, therefore, liquid NaCl is expected to wet the solid Zr and B particles due to capillary forces and then fusion of Zr and B may take place prior to reaction; most probably forming a melt composed of NaCl–Zr–B. System can be considered homogenous for an instant before the reaction between Zr and B, which results in formation of solid  $ZrB_2$  crystals in the melt, melting point of which are higher than the adiabatic temperatures of the NaCl containing compositions. It is possible for the formed  $ZrB_2$  crystals to deplete Zr and B in their vicinity in the melt and on account of the rapid cooling and solidification of the melt after the passage of the reaction wave, ultrafine individual  $ZrB_2$  particles remain isolated. The mechanism is similar to solution-precipitation mechanisms, however, in the presence of a non-reactive liquid phase. The hindrance of mass transport among the  $ZrB_2$  crystals after they are formed is believed to be the basis of the grain refinement effect of NaCl. Indeed, according to the TEM analyses reported by Nersisyan et al.,<sup>12</sup> in the case of SHS formation of TiC from Ti and C in the presence of NaCl, formed TiC particles were mainly separated from each other by a thin layer of NaCl. Although experimental data confirming the presence of Zr and B within the NaCl

matrix prior to reaction is not present, the faceted structure of the formed  $ZrB_2$  particles as seen in Fig. 4(c) is in support of the above discussed mechanism, since solution-precipitation growth mostly leads to faceted particle morphology.<sup>21</sup> In addition, other possible mechanisms such as gas phase reactions are not excluded.

#### 4. Conclusion

Preparation of nano-size  $ZrB_2$  powder via SHS was demonstrated by adding 10–50 wt.% NaCl into Zr–B elemental starting powder. Reactions took place completely even with high NaCl content. Adiabatic temperature of reactions, reaction wave velocity, average crystallite size and particle size of the formed  $ZrB_2$  decreased significantly with increasing NaCl content. 30 wt.% NaCl addition was found to be the optimum and obtained  $ZrB_2$  particles were mostly finer than 200 nm. Hindrance of mass transport among  $ZrB_2$  crystals is believed to be the basis of grain refinement effect of NaCl.

Obtaining nano-sized powder was considered very difficult in SHS due to inevitable high temperatures. Owing to the introduction of NaCl into SHS, process control and preparation of ceramic powder having nano-sized particles were rendered possible. The development has the potential to enrich the spectrum and the properties of materials that could be produced via SHS.

#### Acknowledgements

HEC is grateful to the entire staff of Physicochemistry Department of University of Pavia for providing him the opportunity to study in their department as a visiting scientist, and for their help. His stay was funded by the State Planning Organization of Turkey via Academic Human Resources Program (ÖYP-DPT). Help of Prof. Dr. Ertuğrul Arpaç and Savaş Güven on particle size measurements is gratefully acknowledged. HEC also thanks to Akdeniz University Research Fund for financial support.

#### References

1. Brotherton, R. J. and Steinberg, H., *Progress in Boron Chemistry*, vol. 2. Pergamon Press, New York, 1970.
2. Fahrenholtz, W. G., Hilmas, G. E., Talmy, I. G. and Zaykoski, J. A., Refractory diborides of zirconium and hafnium. *J. Am. Ceram. Soc.*, 2007, **90**, 1347–1364.
3. Monticelli, C., Zucchi, F., Pagnoni, A. and Colle, M. D., Corrosion of a zirconium diboride/silicon carbide composite in aqueous solutions. *Electrochim. Acta*, 2005, **50**, 3461–3469.
4. Munir, Z. A., Synthesis of high-temperature materials by self-propagating combustion methods. *Am. Ceram. Soc. Bull.*, 1988, **67**, 342–349.
5. Mishra, S. K., Das, S. and Ramchandrarao, P., Microstructure evolution during sintering of self-propagating high-temperature synthesis produced  $ZrB_2$  powder. *J. Mater. Res.*, 2002, **17**, 2809–2814.
6. Campbell, I. E. and Sherwood, E. M., *High Temperature Materials and Technology*. John Wiley and Sons Inc., New York, 1967, p. 353.
7. Akgün, B., Formation of zirconium diboride and other metal borides by volume combustion synthesis and mechanochemical process. M.Sc. Thesis, Middle East Technical University, Ankara, 2008.
8. Khanra, A. K., Godkhindi, M. M. and Pathak, L. C., Sintering behaviour of ultra-fine titanium diboride powder prepared by self-propagating high-temperature synthesis (SHS) technique. *Mater. Sci. Eng. A*, 2004, **454–455**, 281–287.
9. Cao, G., *Nanostructures and Nanomaterials*. Imperial College Press, London, 2004, pp. 357–358.
10. Khanra, A. K., Pathak, L. C., Mishra, S. K. and Godkhindi, M. M., Self-propagating-high-temperature synthesis (SHS) of ultrafine  $ZrB_2$  powder. *J. Mater. Sci. Lett.*, 2003, **22**, 1189–1191.
11. Khanra, A. K., Pathak, L. C., Mishra, S. K. and Godkhindi, M. M., Effect of NaCl on the synthesis of  $TiB_2$  powder by a self-propagating high-temperature synthesis technique. *Mater. Lett.*, 2004, **58**, 733–738.
12. Nersisyan, H. H., Lee, J. H. and Won, C. W., Self-propagating high-temperature synthesis of nano-sized titanium carbide powder. *J. Mater. Res.*, 2002, **17**, 2859–2864.
13. Weimin, W., Zhengyi, F., Hao, W. and Runzhang, Y., Chemistry reaction processes during combustion synthesis of  $B_2O_3$ – $TiO_2$ –Mg system. *J. Mater. Process. Technol.*, 2002, **128**, 162–168.
14. Bilgi, E., Çamurlu, H. E., Akgün, B., Topkaya, Y. and Sevinç, N., Formation of  $TiB_2$  by volume combustion and mechanochemical process. *Mater. Res. Bull.*, 2008, **43**, 873–881.
15. Setoudeh, N. and Welham, N. J., Formation of zirconium diboride ( $ZrB_2$ ) by room temperature mechanochemical reaction between  $ZrO_2$ ,  $B_2O_3$  and Mg. *J. Alloys Compd.*, 2006, **420**, 225–228.
16. Çamurlu, H. E. and Maglia, F., Synthesis of zirconium diboride–zirconium nitride composite powders by self-propagating high-temperature synthesis. *J. Mater. Sci.*, 2007, **42**, 10288–10295.
17. HSC Chemistry for Windows-Chemical Reaction and Equilibrium Software, Outokumpu Research Oy, Pori, Finland, 1999.
18. Cullity, B. D. and Stock, S. R., *Elements of X-Ray Diffraction*. Prentice Hall, New Jersey, 2001, p. 169.
19. Subrahmanyam, J. and Vijayakumar, M., Self-propagating high-temperature synthesis. *J. Mater. Sci.*, 1992, **27**, 6249–6273.
20. *Handbook of Chemistry and Physics*, 67th ed., CRC Press, Boca Raton, FL., 1987.
21. Huang, L., Wang, H. Y., Li, Q., Yin, S. Q. and Jiang, Q. C., Effect of Ni content on the products of Ni–Ti–B system via self-propagating high-temperature synthesis reaction. *J. Alloys Compd.*, 2008, **457**, 286–291.